International Journal of ChemTech Research
CODEN (USA): IJCRGG, ISSN: 0974-4290, ISSN(Online):2455-9555
Vol.10 No.10, pp 459-473, 2017

Electro-oxidation of ethanol onto Pt/rGO/C, Pt/rGO-G, Pt/rGO-CB/C and Pt/rGO-ZSM/C Composite Carbon-felt Electrode for Fuel Cell Application

Debalina Das[1], Pradip K. Ghosh[1], Basu M. Daas[2]*

[1]Integrated Science Education & Research Centre, Visva-Bharati, Santiniketan, W. B., India.
[2]Department of Chemistry, Government Degree College, Dharmanagar, Tripura, India.

Abstract : Present study reports, electro-oxidation of ethanol onto platinum (Pt) loaded reduced graphene oxide/Carbon-felt (Pt/rGO/C), rGO-graphite/C-felt composite (Pt/rGO-G/C), rGO-carbon black/C-felt, (Pt/rGO-CB/C) and rGO-ZSM-5/C-felt composite (Pt/rGO-ZSM/C) electrodes. GO was synthesized by conventional, simple and green Hummer's Method. rGO-CB, rGO-G and rGO-ZSM was prepared by mechanical mixing at a fixed ratio. From the electrochemical studies, it was found that Pt/rGO-G/C and Pt/rGO-CB/C proved to be a better and more durable electrocatalyst compared to Pt/rGO/C and Pt/C. However, Pt/rGO-ZSM/C proved the best electrocatalyst. Apparent activation energies of ethanol electro-oxidation over these electrodes are found to be in the order of Pt/C < Pt/rGO/C < Pt/rGO-G/C < Pt/rGO-CB/C < Pt/rGO-G/C. CB or G acts as hinders to inhibition of stacking of rGO sheets, as effective "spacers". CB or G have many defects and act as second support material over which PNPs deposited are smaller in size, compared to deposition over bare rGO/C or C-felt surfaces. ZSM-5 enhances the catalytic power of PNPs by facilitating formation of smaller PNPs and also by cleansing away adsorbed CO from the Pt surface. The present study thus will lead to a new avenue in the field of fuel cell electro-catalysts.
Keywords : Fuel cells; Graphene; Carbon; Zeolites; Hybrid composites.

1. Introduction

Platinum loaded reduced graphene oxide (rGO)/C electrodes have catalytic action towards electro-oxidation of ethanol (EtOH) [1]. In this investigation, the possibility of improving those electrodes using carbon black (CB), graphite (G) and ZSM-5 (Z) as support materials was explored. These materials have been reported to improve electrical contact among the components of the composites. This investigation was aimed at the preparation of Pt loaded rGO/C, rGO-G/C, rGO-CB/C and rGO-ZSM/C composite electrodes and an investigation of EtOH electro-oxidation onto these electrodes. EtOH is emerging as an alternative fuel for direct alcohol fuel cells (DAFCs). The major advantages of EtOH are its non-toxic nature and ease of production from biomass etc. In fuel cell research, the conventional Pt and Pt-based materials have been utilized as the foremost catalysts for direct ethanol fuel cells (DEFCs) [2,3]. But for the commercialization of the DEFC and its application, chief obstacles are unaffordable cost of the noble metals as well as the inability of Pt to catalyze the fission of C-C bond and to cleanse the adsorbed CO intermediate [4-6]. Therefore, the alternative path leads to synthesis of non-precious metal as well as metal-free catalysts. Keeping an eye on the maximum utilization of this precious metal and to minimize the cost, high surface area supporting materials are showing new path for better catalyst loading. The perfect support materials should contain high specific surface area,

good electronic conductivity and significant amount of porosity [7,8]. Porous carbon materials, conducting polymers and transition-metal oxides are considered as effective support materials for their porosity [9,10]. Amongst this class, porous carbon materials (e.g. carbon black) are promising due to their high surface, long cycle life and excellent mechanical properties [11,12]. In last decade graphene and rGO nanosheets have been considered with high specific surface area, exceptional graphitized basal plane structure, excellent electrical, mechanical and thermal properties, better transparency, mechanical strength and superb conductivity [13-18]. Another interesting point is, unlike the traditional carbon materials (e.g. activated carbon, carbon nanotubes etc.) the high specific surface area of rGO-Graphene materials are independent of the allocation of the pores in solid state. It is exclusively reliant on the interrelated open channels amongst graphene layers in a 2d manner [19].

However, there are major pitfalls to obstruct the application of rGO as a support material. The 2d material the rGO sheets are prone to pile together due to strong affinity for π-π interaction of the individual sheets which blocks the catalytic sites, gives rise to a major loss of the effective surface area of rGO, causes a higher resistance for the diffusion of reactant molecules on the catalyst surface and sluggish the catalytic reaction [20-22]. It was further observed that during the drying process, the individual rGO-Graphene sheets leads to irreversible agglomeration or restacking by means of van der Waals interactions [23,24]. The rGO sheets obtained by conventional methods possess more defects which hinder the electron transfer rate in the rGO sheet as well as across the Rgo nanocomposite interface. Lastly, rGO-Graphene with basal layers is unfavorable for dispersion of electrolyte within the layers [25,26]. This adverse phenomenon hinders the application of these materials in fuel cell or other energy devices.

To overcome the stacking trouble of the individual rGO sheets, insertion of a second support material within the individual sheets proved to be a constructive and green method. The inclusion of a second support material not only improves the homogeneous dispersion of rGO sheets but also lowers the defects. Carbon black (CB) and graphite (G) are most useful second support material with higher electrochemical surface area (ECSA) and good electronic conductivity [11,12,27-29]. The assimilation of CB or graphite within rGO layers can prominently control the agglomeration or restacking of individual sheets and enhances the electrolyte–electrode convenience as well as electrode conductivity. Some productive consequences of insertion of CB-G particles are amplification of spacing between the rGO sheets and a swift diffusion path for more edge plane involvement [10]. As an result, the CB-G as spacers gives rise to high electrochemical exploitation of rGO layers and also opens up nanochannels constructing 3d rGO-CB or rGO-G hybrid material [12,27]. The composite support materials can be synthesized by easy and in a greener way.Some momentous works regarding synthesis and application of rGO-CB or rGO-G hybrid materials are worth discussing. Yan et al. have synthesized Graphene nanosheets and carbon black composite by ultrasonication followed by in-situ reduction methods [11]. They have examined that electrochemical performances of hybrid materials are superiorto the pure graphene material, and proved that carbon black particles as spacers ensured the high electrochemical utilization of graphene layers. Li et al. had synthesized CB, Pt loaded rGO composite catalyst for oxygen reduction reaction (ORR) study [27]. They have revealed that the inclusion of CB particles between rGO sheets can effectively prevent stacking of rGO, promoting diffusion of oxygen molecules through the rGO sheets and enhancing the ORR electro-catalytic activity. Shervedani et al. prepared sulphur doped graphene nanosheets (S-GNS)-CB composite catalyst for ORR study [12]. Their outcome proved that CB particles inserted between S-GNs layers function as spacers and prevent the restacking of S-GNs during drying, endorse the diffusion of O_2 molecules through S-GNs and increase the ORR rate. Yuan et al. have synthesized a 3d graphene oxide/carbon sphere supported silver composite (Ag-GO/C) catalyst for ORR [30]. They have established that the enhancement can be demonstrated to the 3D composite support, which supplement the electrical conductivity by implementing the mass transport in the catalyst layer aided the reactants access to the active sites. In a different study, Li et al. have prepared reduced graphene oxide (rGO) activated carbon (AC) composites rGO-AC by a facile chemical method and applied in the capacitive removal of salt ions from brackish water [31]. They have seen that rGO can act as a flexible bridge to form a ‘‘plane-to-point’’ (rGO- AC) conducting network, which effectively weaken the aggregation of AC particles. As a result it advances the electron transfer within the composite electrode. In recent past, researchers have significantly synthesized rGO-G composite support materials for various energy devices. In a pioneer study, Zhang et al. have fabricated a composite of graphite and graphene oxide and employed as a high capacity and binder-free anode material directly in lithium-ion batteries [29]. They observed that the graphite particles and conductive additive homogeneously distributed on the graphene oxide surface and the oxygen containing groups of graphene oxide also have been partially reduced during the first discharge process. In their next study, Zhang et al. have synthesized a composite of graphene oxide sheets, carbon

nanotubes (CNTs), and commercial graphite particles and utilized as binder-free anode material for Li-ion batteries [28,29]. They concluded that this graphene oxide/graphite/CNT composite had finer reversible capacity, improved cycling performance, and similar rate capability compared to the GO/graphite composite.

Again, Zeolites, specially ZSM-5 which has been studied also can act as a second catalyst as it has inbuilt ability to cleanse the electrode surface during electro-oxidation process by oxidizing adsorbed CO to CO_2 [6,32]. Zeolites are crystalline aluminosilicates with linked tetrahedra, each tetrahedron containing four O atoms around a cation. Zeolites have a network of channels and sieves [33-35]. Zeolites nanoparticles are good quality supporting catalyst and adsorbent material due to their bulky surface area, small diffusion path lengths and readily accessible active sites [36-42]. Easily prepared and low cost zeolite-modified electrodes are a subcategory of chemically modified electrodes, which were probed by the research groups of Baker, Calzaferri, Devynck, Mallouk, Murray, Phani, Rolison, Shaw and Walcarius[43-48].

In the present study rGO-CB and rGO-G composite support materials have been synthesised using a facile and greener technique by ultra-sonication and electro-chemical reduction process. Pt nanoparticles (PNPs) have been electro-deposited over bare rGO/C, rGO-G/C, rGO-CB/C and rGO-ZSM/C. Comparative energies of activation for EtOH electro-oxidation have been calculated over Pt/C, Pt/rGO/C, Pt/rGO-G/C, Pt/rGO-CB/C and Pt/rGO-ZSM/C electrodes taking cyclic voltammograms within temperature range 283-313 K. Chronoamperometric studies have been carried out to determine the catalyst durability. Thus the current study will lead an insight on how the CB or G acts in enhancing the activity of rGO as well as the Pt catalyst towards EtOH electro-oxidation.

2. Materials and Methods

2.1. Chemicals and Reagents used

Carbon black, Graphite powder and H_2PtCl_6 were acquired from Alfa-Aeser (India). ZSM-5 was procured from Greenstone, Switzerland. Other chemicals for example $KMnO_4$, $NaNO_3$, H_2SO_4, HCl, and 30% H_2O_2 were obtained from Merck (India).

2.1. Preparation of graphene oxide

Graphite oxide was synthesized by conventional Hummer's Method [49]. Graphene oxide was fabricated by taking 0.025 g graphite oxide in 50 ml deionized water and subjected to ultrasonication for 1 h for exfoliation. The as prepared homogeneous mixture was centrifuged at 3000 rpm for 30 min. A non-sediment supernatant solution was obtained after decanting it and the residue was thoroughly washed with deionized water and vacuum dried overnight.

2.2. Preparation of composites

The GO-CB, GO-G and GO-ZSM mixtures (5:1 ratio) were taken in a solution of Nafion 117, isopropyl alcohol and distilled water(0.001 $g.mL^{-1}$)and each were stirred vigorously for 1h. Next the individual mixtures were exfoliated by means of ultrasonication for 3h in an ultrasonic bath (KQ-600KDE, 600W). The resulting homogeneous dispersions were mixed with 0.5M H_2SO_4 solution and then refluxed for 24h in room temperature (298K). Finally the composites were centrifuged at 3000 rpm for 30 min to get non-sediment supernatant solution and washed several times with deionized water.

2.3. Preparation of electrodes

The prepared GO, GO-CB, GO-G and GO-ZSM composites were sprayed by a sprayer over carbon felt (C-felt) surface (1 cm length × 1 cm width, 2.4 mm thickness, 0.95 porosity, mean fibre diameter of 20 µm, electrical conductivity 10 S/m) and the loaded C-felts were vacuum dried overnight. These composites were electrochemically reduced to rGO-CB, rGO-G and rGO-ZSM on a bath containing 0.5 M H_2SO_4 solution, by passing a current of (-)1 $mA.cm^{-2}$ for 30 min and washed thoroughly by deionized water.

Pt was deposited electro-chemically over bare C-felt, rGO/C, rGO-G/C, rGO-CB/C and rGO-ZSM surfaces galvanostatically by passing a current of (-)1 $mA.cm^{-2}$ for 100 s. The four electrodes were kept in separate baths in a series, each of which contains plating electrolyte of 2×10^{-3} M solution of chloroplatinic acid

($H_2PtCl_6.6H_2O$) in 1.0 M H_2SO_4. The initial and final weights of the prepared electrodes are recorded to calculate the mass activity (MA) in $mA.mg^{-1}$.

The Pt/C, Pt/rGO/C, Pt/rGO-G/C, Pt/rGO-CB/C and Pt/rGO-ZSM/C electrodes were used as anode catalysts for EtOH electro-oxidation.

3. Characterization

Fourier Transform Infra-red Spectroscopy (FTIR) of Pt/rGO/C, Pt/rGO-G/C, Pt/rGO-CB/C and Pt/rGO-ZSM/C have been taken using Shimadzu FTIR 8400 S. The powder XRD diffraction of Pt/rGO/C, Pt/rGO-G/C, Pt/rGO-CB/C and Pt/rGO-ZSM/C were done by employing Rigaku Ultima IV fitted with miniflex goniometer and Cu target by continuous scanning with 30 kV/15 mA X-ray on a standard sample-holder with 4.2^0 scattering slit and 0.3 mm receiving slit, at scanning mode of 2θ through a Kb filter. The surface morphology of the Pt/rGO/C, Pt/rGO-G/C, Pt/rGO-CB/C and Pt/rGO-ZSM/C electrodes were taken by transmission electron microscope (TEM) (FEI TECNAI 200 KV) and scanning electron microscope (SEM) (Hitachi S-3000 N and Jeol-JSM-6390). For TEM analysis, the corresponding electrode materials were dispersed in EtOH and subjected to ultrasonication for 10 min. A few drops of the suspensions were deposited onto TEM grid and evacuated before analysis.

Electrochemical studies have been carried out using a three electrode cell by a potentiostat–galvanostat (by PAR VersaStatTM II). A Pt-foil (1 cm^2) was utilized as a counter electrode and a saturated calomel electrode as reference electrode, respectively. A solution of 1 M EtOH, in 0.5 M H_2SO_4 was taken as electrolytic bath. Cyclic voltammetry experiments were carried out at four different scan rates: 0.01, 0.03, 0.05 and 0.07 $V.s^{-1}$ and within a temperature range (283-313 K).

4. Results

4.1. Characterization of electrodes

4.1.1. FTIR spectral analysis of the electrodes

FTIR spectra of Pt/rGO/C, Pt/rGO-CB/C and Pt/rGO-G/C show considerably suppressed characteristic bands of oxygenic functional groups (–OH stretching vibrations at 3600-3400 cm^{-1} and -C=O stretching vibration at 1753 cm^{-1}) (Figure 1).

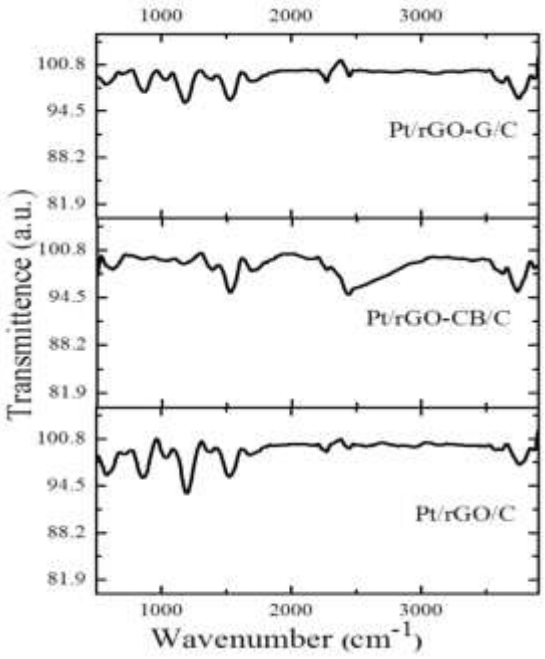

Figure 1.FTIR spectra of Pt/rGO/C, Pt/rGO-CB/C and Pt/rGO-G/C.

This indicates a successful reduction of GO to rGO in electrochemical means. The absorption bands at 1500-1550 cm^{-1} can be assigned as the skeletal vibration of the graphene sheets. A peak at approximately 1150-1200 cm^{-1} points out that the GO in Pt/rGO, Pt/rGO-CB/C and Pt/rGO-G/C nanocomposites were effectively deoxygenated and reduced. It also indicates the stretching vibrations of the phenolic and carboxylic groups from the reduced GO sheets [12,30] In the FTIR spectrum for shows a characteristic lump at 2500 cm^{-1} most propably due to C-H vibrations [50-52].

4.1.2. Powder XRD analysis of the electrodes

Powder XRD patterns of the Pt/rGO/C, Pt/rGO-G/C, Pt/rGO-CB/C and Pt/rGO-ZSM/C show diffraction peak at 2θ = 40° corresponding to the Pt (111) face centered cubic (fcc) lattice (Figure 2).

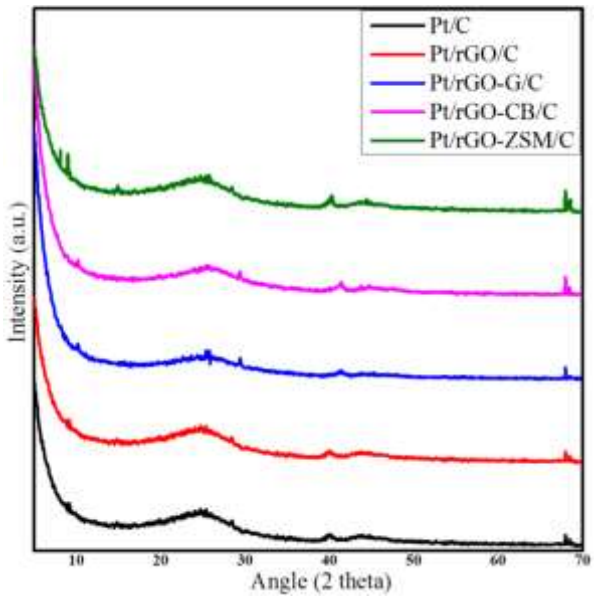

Figure 2.Powder XRD of Pt/rGO/C, Pt/rGO-G/C, Pt/rGO-CB/C and Pt/rGO-ZSM/C.

The shifted towards higher value of 2θ = 41.3° and 41.4° as smaller sized platinum nanoparticles (PNPs) are formed. The peak at 2θ = 43.8° represent the Pt(200) nanoparticles. On the other hand, the peak at 2θ = 68.1° confirms the Pt(220) fcc lattice. The peaks at 2θ = 44.7°, 44.8°, 68.5° and 68.6° are due to smaller PNPs [53-56].

The wide peaks at 2θ = 24.7°, 25.8° and 25.4° confirm the graphitic nature of rGO sheets which indicate partial reduction of GO into rGO. The peak at 2θ = 68° represent the Pt(200) nanoparticles formed in case of Pt/rGO-ZSM/C. [57-59].

All those data indicated formation of fcc structures of the platinum crystal over Pt/rGO/C, Pt/rGO-G/C, Pt/rGO-CB/C and Pt/rGO-ZSM/C surfaces.

4.1.3. SEM-EDX & TEM analysis of the electrodes

SEM micrographs of PNPs deposited onto rGO/C, rGO-G/C, rGO-CB/C and rGO-ZSM/C (Figure 3) clearly indicates that the PNPs deposited over rGO-CB/C and rGO-G/C are smaller in size compared to rGO/C. On the other hand some PNPs over rGO/C get agglomerated and take bigger size. In Pt/rGO-ZSM/C PNP deposition takes place on the conductive rGO and not on the external or internal surface of ZSM-5 [48].

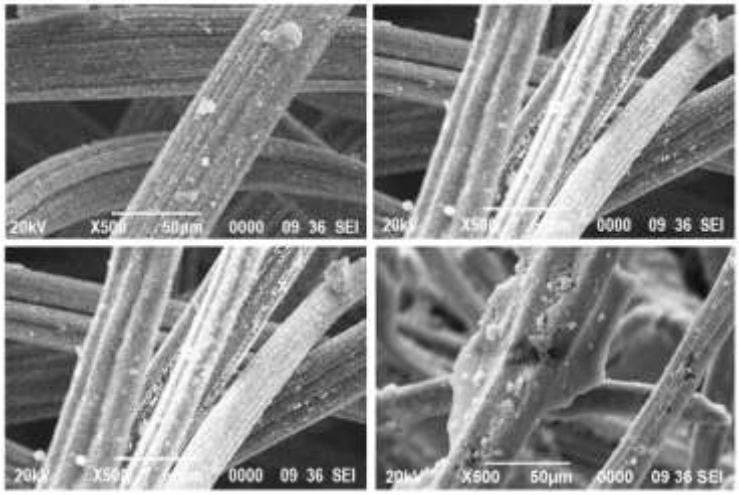

Figure 3.SEM micrographs of Pt/rGO/C, Pt/rGO-G/C, Pt/rGO-CB/C and Pt/rGO-ZSM/C.

The energy dispersive X-Ray (EDX) patterns of Pt/rGO/C, Pt/rGO-G/C, Pt/rGO-CB/C and Pt/rGO-ZSM/C composites show the corresponding peaks of C, O and Pt elements, which confirmed the deposition of PNPs over rGO/C, rGO-G/C, rGO-CB/C and rGO-ZSM/C nanosheets (Figure 4).

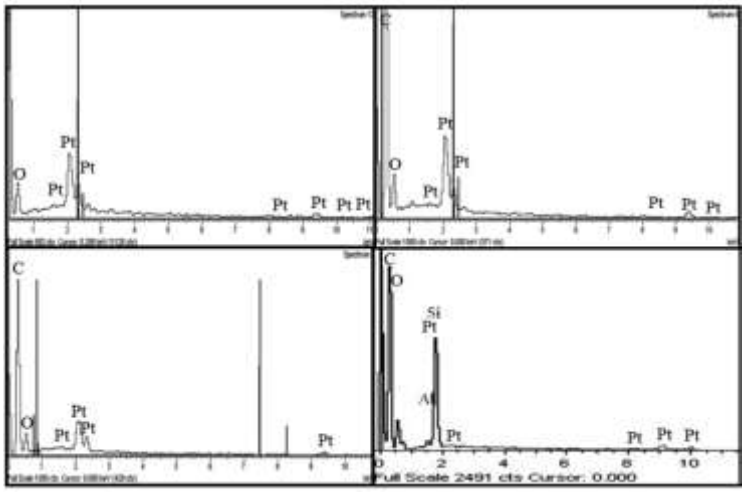

Figure 4. EDX patterns of Pt/rGO/C, Pt/rGO-G/C, Pt/rGO-CB/C and Pt/rGO-ZSM/C

TEM micrographs of PNPs electro-deposited onto rGO, rGO-CB, rGO-G and rGO-ZSM surfaces reveal that rGO, rGO-CB, rGO-G and rGO-ZSM composite support materials effect on the morphology and size of the PNPs (Figure 5).

In rGO/C, rGO-G/C, rGO-CB/C and rGO-ZSM/C composites the PNPs deposited are in the size range 10-30 nm, 10-15 nm, 10-15 nm and 5-6 nm respectively as estimated by imageJ software [60,61].It is a well-established fact that performance and morphology of Pt nanosized catalysts is influenced by the nature and structure of the support materials [13,14]. The diffusion co-efficient (D) of Pt electro-deposition varies with different support materials. The larger the D value, the faster is the deposition [56].

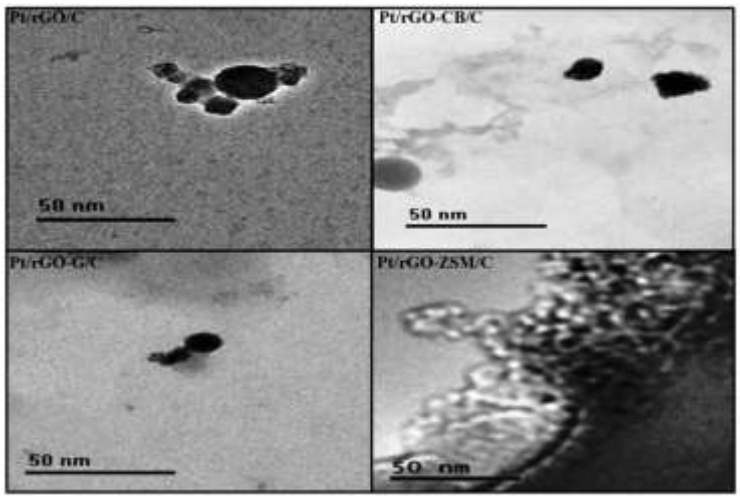

Figure 5.TEM micrographs of PNPs electro-deposited onto Pt/rGO, Pt/rGO-CB, Pt/rGO-G and Pt/rGO-ZSM.

Many researchers have proved that size and shape controlled metallic nanoparticles supported onto mesoporous materials are liable in altering catalytic activity and substrate selectivity [15,16].

4.2. Electrochemical studies

4.2.1. Electrochemically active surface area analysis of the electrodes

Electrochemically active surface area (EAS) is useful in determining the electrochemically active sites per gram of the catalyst [58,62]. It plays an important role in distinguishing the activity between different electro-catalytic materials. To determine the EAS of Pt/C, Pt/rGO/C, Pt/rGO-CB/C and Pt/rGO-G/C electrodes, cyclic voltammograms were recorded in 0.5 M H_2SO_4 solution within potential range -0.3 to 1.0 V with a scan rate 50 $mV.s^{-1}$ (Figure 6).

The Electrochemically active surface area (EAS) values calculated were in the order of Pt/C (15.4 $m^2.g^{-1}$) < Pt/rGO/C (69 $m^2.g^{-1}$) < Pt/rGO-CB/C (77 $m^2.g^{-1}$) < Pt/rGO-G/C (86.5 $m^2.g^{-1}$) < Pt/rGO-ZSM/C (99.5 $m^2.g^{-1}$) in the ratio of 4.5: 5: 5.6: 6.5 compared to bare Pt/C. Presence of PNPs on the electrodes is evident from the downward lumps in the potential range of 0.5 to 0.6 V in all the cases except Pt/C; which is due to reduction of oxidized PNPs deposited.

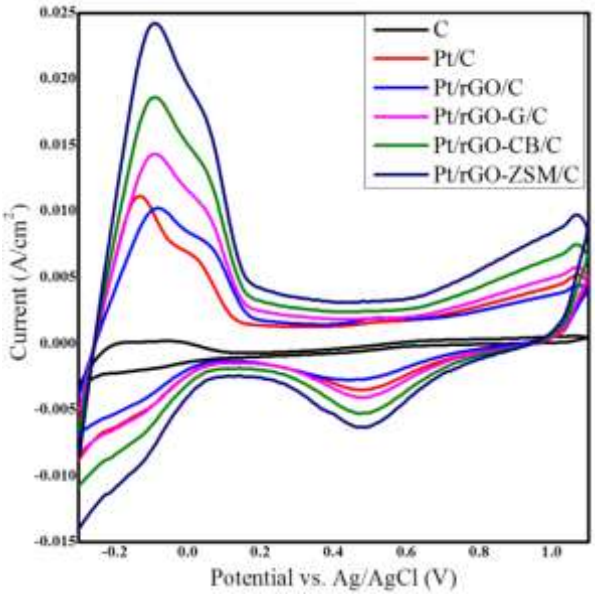

Figure 6.EAS of Pt/C, Pt/rGO/C, Pt/rGO-CB/C and Pt/rGO-G/C.

The broad peaks on the left in the potential range of -0.1 to 0.0 V is due to hydrogen adsorption and desorption [63-67]. Electrochemically active surface area is the maximum in case of Pt/rGO-ZSM/C justifying that smaller PNPs were deposited, facilitating more surface area exposure.

4.2.2. Cyclic voltammetric analysis of the electrodes

The electro catalytic activities of Pt/rGO-G/C, Pt/rGO-CB/C, Pt/rGO/C and Pt/C for EtOH (1.0 M in 0.5 M H2SO4) electro-oxidation were evaluated by cyclic voltammetry study at 308 K and at a scan rate 50 $mV.s^{-1}$ (Figure 7).

It was observed that all the electrodes exhibit similar anodic peaks in the forward scan and reverse scan for EtOH electro-oxidation; only in case of Pt/rGO-ZSM/C the peak in the reverse scan occurs at a higher potential. Earlier it was thought that the back peak indicated the oxidation of CO or residual carbonaceous species.

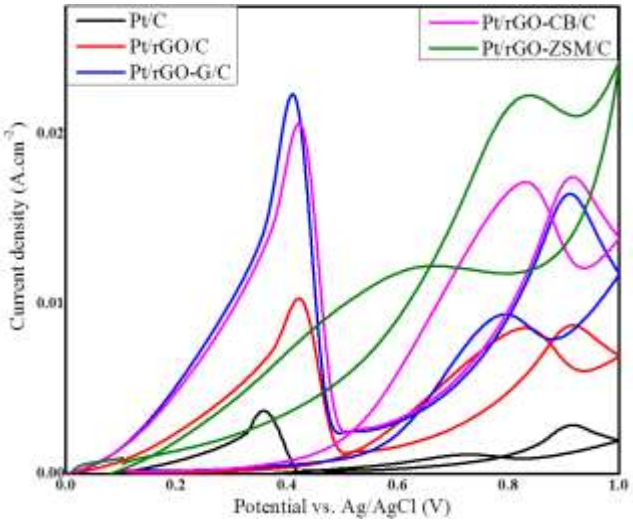

Figure 7. Cyclic voltammetry of Pt/C, Pt/rGO/C, Pt/rGO-G/C, Pt/rGO-CB/C and Pt/rGO-ZSM/C catalysed EtOH electro-oxidation.

But recent research proved that the back peak is not due to oxidation of adsorbed CO but due to the EtOH electro-oxidation itself on Pt-O_x. Pt is oxidized to Pt-O_x, and then Pt reduction potential is negatively shifted. With the formation of Pt-O_x the available surface area of Pt is reduced thus lowering the back peak. In all the cases, the forward and backward peaks intersect as in EtOH electro-oxidation the backward peaks are prominent due to EtOH electro-oxidation over P-O_x [68].

Comparing the cyclic voltammograms of these electrodes for EtOH oxidation, it was found that the forward peak current densities (I_F) were enhanced by 3, 5.8, 6.1 and 7.8 times over Pt/rGO/C, Pt/rGO-G/C, Pt/rGO-CB/C and Pt/rGO-ZSM/C compared to bare Pt/C respectively. The MA in $mA.cm^{-1}$ calculated also follows the order Pt/C < Pt/rGO/C < Pt/rGO-G/C < Pt/rGO-CB/C < Pt/rGO-ZSM/C. Thus, the elevated values of I_F and MA over Pt/rGO-ZSM/C compared to others indicates better catalytic behavior of the zeolite modified electrode.

4.2.3. Arrhenius plots analysis of the electrodes

Arrhenius plots for Pt/C, Pt/rGO/C, Pt/rGO-G/C, Pt/rGO-CB/C and Pt/rGO-ZSM/C catalysed EtOH electro-oxidation were drawn by calculating apparent rate constant values using the equation, i = n.F.k [1,59,69].

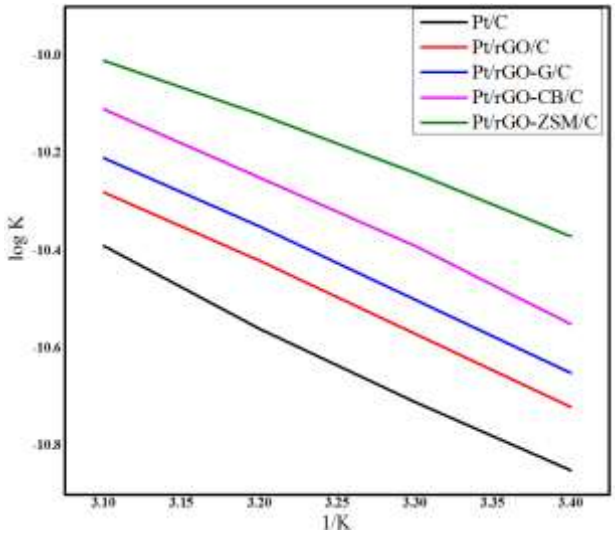

Figure 8.Arrhenius plots for Pt/C, Pt/rGO/C, Pt/rGO-G/C, Pt/rGO-CB/Cand Pt/rGO-ZSM/C catalysed EtOH electro-oxidation.

The forward anodic current values for EtOH electro-oxidation over these electrodes were taken at a fixed potential 0.6 V, individually within the temperature range of 283-313 K. All the current values were normalized with respect to the EAS values and catalyst loading factor (expressed as $i.cm^2.mg^{-1}$). The apparent rate constant (k) values were calculated from the equation i = n.F.k where n = No. of electrons involved in the electro-oxidation process (n = 12 for EtOH assuming complete oxidation), F= Faraday constant, i = Average current density over all scan rate at 0.6 V [2].

Typical Arrhenius plots for these individual electrodes were obtained by plotting log k ($k/mol.cm^{-2}.s^{-1}.mg^{-1}$) vs. 1/T (Figure 8) [1,59,69].

The apparent activation energy values were computed from the slopes of these curves (Table 1).

Table 1.Apparent activation energy values of EtOH electro-oxidation (E = 0.6 V) over Pt/C, Pt/rGO/C, Pt/rGO-G/C, Pt/rGO-CB/C and Pt/rGO-ZSM/C electrode surfaces.

Electrode	Slope	Activation energy
Pt/C	-1.7	33
Pt/rGO/C	-1.55	29.5
Pt/rGO-G/C	-1.42	26.5
Pt/rGO-CB/C	-1.5	28
Pt/rGO-ZSM/C	-1.37	25.1

It was found that activation energies for EtOH electro-oxidation for these electrodes were in the order Pt/rGO-CB/C ($26.5kJ.mol^{-1}$) < Pt/rGO-G/C ($28kJ.mol^{-1}$) < Pt/rGO/C ($29.5kJ.mol^{-1}$) < Pt/C ($33\ kJ.mol^{-1}$). This indicated better catalytic activity of Pt/rGO-CB/C and Pt/rGO-G/C electrodes compared to Pt/rGO/C and Pt/C electrodes.

4.2.4. Chronoamperometric analysis of the electrodes

Chronoamperometric analysis is very useful in establishing the durability of the catalyst and its anti-poisoning activity [69]. The durability of the catalysts can be roughly judged by steady current densities referred in the amperometric i-t curves.

Steady state amperometric study for electro-oxidation of 1.0 M EtOH in 0.5 M H_2SO_4 over Pt/C, Pt/rGO/C, Pt/rGO-G/C, Pt/rGO-CB/C and Pt/rGO-ZSM/C electrodes were carried out at a fixed potential of 0.4 V (Figure 9).

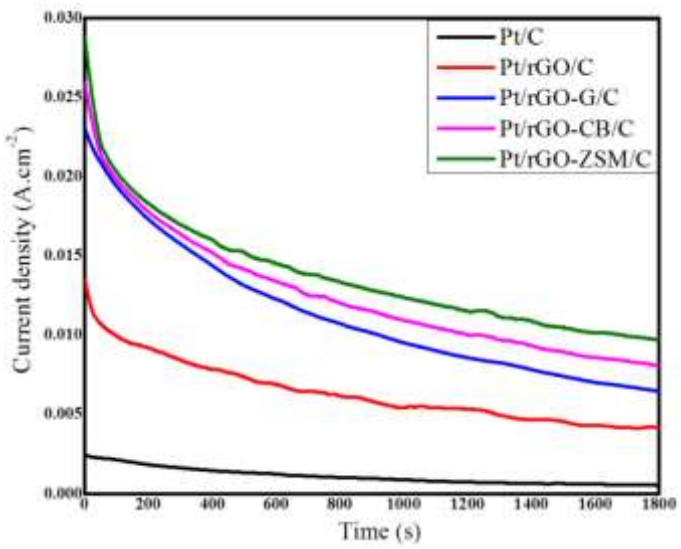

Figure 9.Chronoamperometry of Pt/C, Pt/rGO/C, Pt/rGO-G/C, Pt/rGO-CB/C and Pt/rGO-ZSM/C catalyzed EtOH electro-oxidation.

The surface area of each electrode was maintained 1 cm^2 and the reaction conditions were also kept identical. Current decays are also concurrent with the inhibition towards catalyst surface poisoning by the intermediate carbonaceous species [65]. It was found that deactivation of Pt was significantly reduced in Pt/rGO-G/C, Pt/rGO-CB/C and Pt/rGO-ZSM/C electrodes. The Pt/rGO-G/C, Pt/rGO-CB/C and Pt/rGO-ZSM/C composite catalyst exhibited steady nature of the curves with time maintaining greater current density both at the initial state and at the end within the time range studied compared to that of Pt/rGO and bare Pt. The Turn-over number (TON) for the above catalysts were calculated from the current density at 1800s using the equation,

$$\text{TON} = \text{Molecules/Sites} = (i \times 6.023 \times 10^{23})/(nF \times 1.3 \times 10^{15})$$

where i= Steady-state current density at 1500s of scanning, n is the number of electrons produced by oxidation of 1.0 M EtOH which is 12, F = Faraday constant (96,487 C), and 1.3×10^{15} cm^{-2} = Density of the topmost atoms of an ideal Pt(100) surface [64].

Thus TON of the catalysts increased in the order Pt/C < Pt/rGO/C <Pt/rGO-G/C < Pt/rGO-CB/C < Pt/rGO-ZSM/C which shows that the capability of the catalysts also followed the same order.

4.2.5. Potentiodynamic polarization analysis of the electrodes

E vs. i data of the Pt/C, Pt/rGO/C, Pt/rGO-G/C, Pt/rGO-CB/C and Pt/rGO-ZSM/C electrodes were obtained and Tafel plot was plotted (Figure 10).

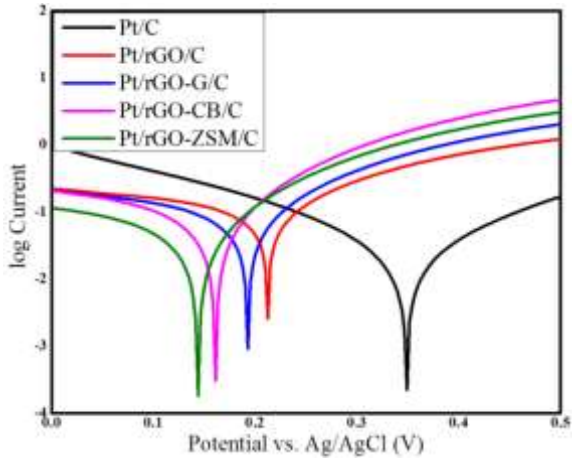

Figure 10.Tafel plots ofPt/C, Pt/rGO/C, Pt/rGO-G/C, Pt/rGO-CB/C and Pt/rGO-ZSM/C.

According to the Tafel equation [70], the values of i_0 is increased in the order of Pt/C < Pt/rGO/C <Pt/rGO-G/C < Pt/rGO-CB/C < Pt/rGO-ZSM/C electrodes. It indicates that the coexistence of GO can accelerate the process of EtOH electro-oxidation but it is more facilitated by the addition of spacers like G, CB and ZSM-5. Again, coexistence of ZSM-5 increases the catalysis of EtOH electro-oxidation more than CB and G. The open circuit potential of EtOH oxidation is decreased in the order of Pt/C < Pt/rGO/C <Pt/rGO-G/C < Pt/rGO-CB/C <Pt/rGO-ZSM/C electrodes. It implies that the ease of electro-oxidation of EtOH at the electrodes is in the order of Pt/C < Pt/rGO/C <Pt/rGO-G/C < Pt/rGO-CB/C <Pt/rGO-ZSM/C electrodes.

5. Discussion

All these data indicated that Pt/rGO-G/C, Pt/rGO-CB/C and Pt/rGO-ZSM/C composite electrodes showed better electro-catalytic activity and enhanced catalytic durability compared to Pt/rGO or bare Pt catalyst. This phenomenon can be explained by different approaches. One elucidation is that the incorporation of CB or G within the rGO sheets can effectively restrain the agglomeration of rGO sheets. It also advances the electrolyte electrode interactions and also augments electrode conductivity. Another hypothesis is that, in the hybrid structure of Pt/rGO-CB or Pt/rGO-G the stretchy 2d contour of rGO sheets may act as a "network" that avert the leaching of dissolved Pt species into the electrolyte [27]. Simultaneously CBs can provide an active site for re-confine or re-nucleation of small Pt clusters. It was a well-established fact that defects or kinks over the active support surface can hand out as heterogeneous nucleation sites [72,73]. In contrast with a smooth graphitized surface, CB surface possesses kinks and traps, which supplies more nucleation sites for migrating Pt species. So, CB effectively captures more migrating Pt species. It was also monitored that the size of PNPs deposited over CB is smaller than that of deposited over bare rGO sheets. Again ZSM-5 itself acts as a second catalyst to PNPs and also facilitates further electro-oxidation by cleansing the metal surface from adsorbed CO [6,32]. All these facts confirm the role of the spacers like rGO-G and rGO-CB and second supporting catalyst rGO-ZSM composites in enhancing the catalytic activity and durability.

6. Conclusion

The present study puts forward some attractive outcomes regarding the Pt/rGO-G/C, Pt/rGO-CB/C and Pt/rGO-ZSM/C composite catalysts for EtOH electro-oxidation. The composite materials were synthesized by user friendly and greener way. From the study, it is interestingly found that Pt/rGO-G/C, Pt/rGO-CB/C and Pt/rGO-ZSM/C composite catalysts show lower energy of activation compared to Pt/rGO or bare Pt catalysts. Moreover, the composite electrodes, Pt/rGO-G/C and Pt/rGO-CB/C, proved more durable than the other two. But the zeolite modified electrode Pt/rGO-ZSM/C I found to the comparatively the best catalyst in terms of activity as well as durability.

The findings can be summarized as:

a. CB or G acts as hinders to inhibition of stacking of rGO sheets, as effective "spacers".

b. CB or G have many defects and act as second support material over which PNPs deposited are smaller in size, compared to deposition over bare rGO/C or C-felt surfaces.
c. ZSM-5 enhances the catalytic power of PNPs by facilitating formation of smaller PNPs and also by cleansing away adsorbed CO from the Pt surface.

The present study thus will lead to a new avenue in the field of fuel cell electro-catalysts.

References

1. Das D., Basumallick I., Ghosh S., Methanol and Ethanol Electro-oxidation on to Platinum Loaded Reduced Graphene Oxide Surface for Fuel Cell Application, British J. Appl. Sci. Tech. 7(6) (2015) 630-641.
2. Zhou W., Zhou Z., Song S., Li W., Sun G., Tsiakaras P., Xin Q., Pt based anode catalysts for direct ethanol fuel cells, Appl. Catal. B, 2003, 48(6), 273-285.
3. Tayal J., Rawat B., Basu S., Bi-metallic and tri-metallic Pt–Sn/C, Pt–Ir/C, Pt–Ir–Sn/C catalysts for electro-oxidation of ethanol in direct ethanol fuel cell, Int. J. Hydrog. Energ., 2012,37(5), 4597-4605.
4. Léger J.M., Rousseau S., Coutanceau C., Hahn F., Lamy C., How bimetallic electrocatalysts does work for reactions involved in fuel cells?: example of ethanol oxidation and comparison to methanol,Electrochim. Acta,2005, 50(25-26), 5118-5125.
5. Lamy C., Rousseau S., Belgsir E.M., Coutanceau C., Leger J.M., Recent progress in the direct ethanol fuel cell: development of new platinum–tin electrocatalysts,Electrochim. Acta, 2004, 49(22-23), 3901-3908.
6. Pang H., Chen J., Yang L., Liu B., Zhong X., Wei X., Ethanol electrooxidation on Pt-ZSM-5 zeolite-C catalyst, J. Solid State Electrochem., 2008, 12, 237-243.
7. Chai G.S., Yoon S.B., Yu J., Ordered porous carbons with tunable pore sizes as catalyst supports in direct methanol fuel cell, J. Physical Chem. B, 2004, 108(22), 7074-7079.
8. Nam J., Jang Y., Kwon Y., Direct methanol fuel cell Pt–carbon catalysts by using SBA-15 nanoporous templates, Electrochem. Commun., 2004, 6(7), 737.
9. Zhao H., Li L., Yang J.,Nanostructured polypyrrole/carbon composite as Pt catalyst support for fuel cell applications, J. Power Sources, 2008, 184(2), 375-380.
10. Huang S.Y., Ganesan P., Park S., Popov B.N.,Development of a titanium dioxide-supported platinum catalyst with ultrahigh stability for polymer electrolyte membrane fuel cell applications, J. Am. Chem. Soc., 2009, 131(39), 13898-13899.
11. Yan J., Wei T., Shao B., Ma F., Fan Z., Zhang M., Zheng C., Shang Y., Qian W., Wei F., Electrochemical properties of graphene nanosheet/carbon black composites as electrodes for supercapacitors, Carbon, 2010, 48(6), 1731-1737.
12. Shervedani R.K., Amini A., Carbon black/sulfur-doped graphene composite prepared by pyrolysis of graphene oxide with sodium polysulfide for oxygen reduction reaction,Electrochim. Acta, 2014, 142, 51-60.
13. Geim A.K., Novoselov K.S., The rise of graphene, Nat. Mater., 2007, 6, 183-191.
14. Peng Z., Yang H., Designer Platinum Nanoparticles: Control of Shape, Composition in Alloy, Nanostructure and Electro catalytic Property, Nano Today, 2009, 4(2), 143-164.
15. Tian N., Zhou Z.Y., Sun S.G., Platinum Metal Catalysts of High-Index Surfaces: From Single-Crystal Planes to Electrochemically Shape-Controlled Nanoparticles, J. Phys. Chem. C, 2008, 112(50), 19801–19817.
16. Lee I., Delbecq F., Morales R., Albiter M.A., Zaera F., Tuning Selectivity in Catalysis by Controlling Particle Shape, Nat. Mat., 2009, 8(2), 132-138.
17. Lee I., Morales R., Albiter M.A., Zaera F., Synthesis of Heterogeneous Catalysts with Well Shaped Platinum Particles to Control Reaction Selectivity, Proceed. Nation. Acad. Sci. USA, 2008, 105(40), 15241-15246.
18. Stankovich S., Dikin D.A., Dommett G.H.B., Kohlhaas K.M., Zimney E.J., Stach E.A., Piner R.D., Nguyen S.T., Ruoff R.S., Graphene-based composite materials, Nature, 2006, 442, 282-286.
19. Stoller M.D., Park S., Zhu Y., An J., Ruoff R.S., Graphene-based ultracapacitors,Nano Lett., 2008, 8(10), 3498- 3502.
20. Si Y., Samulski E.T., Exfoliated graphene separated by platinum nanoparticles, Chem. Mater., 2008, 20(21), 6792-6797.

21. Nam B., Lee H.J., Goh H., Lee Y.B., Choi W.S., Sandwich-like graphene nano composites armed with nano needles, J. Mater. Chem., 2012, 22(7), 3148-3153.
22. Liang Y., Wu D., Feng X., Müllen K., Dispersion of graphene sheets in organic solvent supported by ionic interactions, Adv. Mater., 2009, 21(17), 1679-1683.
23. Yang H., Li F., Shan C., Han D., Zhang Q., Niu L., Ivaska A., Covalent functionalization of chemically converted graphene sheets via silane and its reinforcement, J. Mater. Chem., 2009, 19(26), 4632-4638.
24. Zu S.Z., Han B.H., Aqueous dispersion of graphene sheets stabilized by pluronic copolymers: formation of supramolecular hydrogel, J. Phys. Chem. C,2009, 113, 13651-13657.
25. Gómez-Navarro C., Weitz R.T., Bittner A.M., Scolari M., Mews A., Burghard M., Kern K.,Electronic Transport Properties of Individual Chemically Reduced Graphene Oxide Sheets, Nano Lett., 2007, 7(11), 3499-3503.
26. Yoo E., Kim J., Hosono E., Zhou H.S., Kudo T., Honma I.,Large Reversible Li Storage of Graphene Nanosheet Families for Use in Rechargeable Lithium Ion Batteries,Nano Lett., 2008, 8(8), 2277-2282.
27. Li Y., Li Y., Zhu E., McLouth T., Chiu C.Y., Huang X., Huang Y.,Stabilization of high-performance oxygen reduction reaction Pt electro catalyst supported on reduced graphene oxide/carbon black composite, J. Am. Chem. Soc., 2012, 134(30), 12326-12329.
28. Zhang J., Xie Z., Li W., Dong S., Qu M., High-capacity graphene oxide/graphite/carbon nanotube composites for use in Li-ion battery anodes, Carbon, 2014, 74, 153-162.
29. Zhang J., Cao H., Tang X., Fan W., Peng G., Qu M., Graphite/graphene oxide composite as high capacity and binder-free anode material for lithium ion batteries, J. Power Sources, 2013, 241, 619-626.
30. Yuan L., Jiang L., Liu J., Xia Z., Wang S., Sun G.,Facile synthesis of silver nanoparticles supported on three dimensional graphene oxide/carbon black composite and its application for oxygen reduction reaction, Electrochim. Acta, 2014, 135, 168-174.
31. H. Li, L. Pan, C. Nie, Reduced graphene oxide and activated carbon composites for capacitive deionization, J. Mat. Chem. 22(31) (2012) 15556- 15561.
32. Daas B.M., Ghosh S., Fuel cell applications of chemically synthesized zeolite modified electrode (ZME) as catalyst for alcohol electro-oxidation - A review, J. Electroanal. Chem., 2016, 783C, 308–315.
33. Coombs D.S., Recommended nomenclature for zeolite minerals: report of the subcommittee on zeolites of the International Mineralogical Association, Can. Mineral., 1997, 35, 1571-1606.
34. Rolison D.R., Zeolite-Modified Electrodes and Electrode-Modified Zeolites, Chem. Rev., 1990, 90 (5), 867-878.
35. Sun T., Seff K., Silver Clusters and Chemistry in Zeolites, Chem. Rev., 1994, 94(4), 857-870.
36. G. Reding, T. Maurer, B. Kraushaar-Czarnetzki, Comparing synthesis routes to nano-crystalline zeolite ZSM-5, Micropore. Mesopore. Mater., 57 (2003) 83-92.
37. Grieken R.V., Sotelo J.L., Menendez J.M., Melero J.A., Anomalous crystallization mechanism in the synthesis of nanocrystalline ZSM-5, Micropore. Mesopore. Mater., 2000, 39(1-2), 135–147.
38. Li Q., Wang Z., Hedlund J., Creaser D., Zhang H., Zou X., Bons A., Synthesis and characterization of colloidal zoned MFI crystals, Micropore. Mesopore. Mater.,2005, 78, 1–10.
39. Song W., Justice R.E., Jones C.A., Grassian V.H., Larsen S.C., Synthesis, Characterization, and Adsorption Properties of Nanocrystalline ZSM-5, Langmuir, 2004, 20(19), 8301–8306.
40. Kim S.D., Noh S.H., Park J.W., Kim W.J., Organic-free synthesis of ZSM-5 with narrow crystal size distribution using two-step temperature process, Micropore. Mesopore. Mater., 2006, 92(1-3), 181–187.
41. J. Aguado, D.P. Serrano, J.M. Escola, J.M. Rodrıguez, Low temperature synthesis and properties of ZSM-5 aggregates formed by ultra-small nanocrystals, MicroporeMesopore Mater. 75 (2004) 41–49.
42. Frisch S., Rosken L., Caro J., Wark M., Micropore. Mesopore.Mater., 2009, 120, 47–52.
43. Walcarius A., Zeolite-modified electrodes in electroanalytical chemistry, Anal. Chim. Acta, 1999, 384(1), 1–16.
44. Murray R.W., Chemically Modified Electrodes, Acc. Chem. Res., 1980, 13, 135-141.
45. Murray R.W., Ewing A.G., Durst R.A., Chemically modified electrodes molecular design for electroanalysis, Anal. Chem., 1987, 59(5), 379A–390A.
46. Murray R.W., Molecular design of electrodes surfaces, in: Techniques of Chemistry 22, Wiley, New York, 1992.
47. Murray R.W., Goodenough J.B., Albery W.J., Modified Electrodes: Chemically Modified Electrodes for Electrocatalysis [and Discussion], Phil. Trans. R. Soc. Lond., 1981, A 302, 253-265.
48. Senaratne C., Baker M.D., Rolison D.R., Zhang J., Bessel C.A., Zeolite-Modified Electrodes: Intra-

versus Extrazeolite Electron Transfer, J. Phys. Chem., 1996, 100(14), 5849-5862.
49. Hummers Jr. W.S., Offeman R.E., Preparation of graphitic oxide, J. Am. Chem. Soc., 1958, 80, 1339-1339.
50. Ţucureanu V., Matei A., Avram A.M., FTIR Spectroscopy for Carbon Family Study, Crit. Rev. Anal. Chem., 2016, 46(6), 502-520.
51. Park J.H., Choppala G., Lee S.J., Bolan N., Chung J.W., Edraki M., Comparative Sorption of Pb and Cd by Biochars and Its Implication for Metal Immobilization in Soils, Water Air Soil Pollut., 2013, 224(1711), 1-12.
52. J.M. O'Rejllyi, R.A. Posher, Functional groups in carbon black by FTIR spectroscopy, Carbon21(1) (1983) 47-51.
53. Shen Y., Xiao K., Xi J., Qiu X., Comparison study of few-layered graphene supported platinum and platinum alloys for methanol and ethanol electro-oxidation, J. Power Sources, 2015, 278, 235-244.
54. H.P. Klug, L.E. Alexander, X-ray Diffraction Procedures for Polycrystalline and Amorphous Materials, John Wiley & Sons, New Jersey, 1974.
55. Burton A.W., Ong K., Rea T., Chan I.Y., On the estimation of average crystallite size of zeolites from the Scherrer equation: a critical evaluation of its application to zeolites with one-dimensional pore systems, Micropor. Mesopor.Mater.,2009, 117(1), 75-90.
56. Monshi A., Foroughi M.R., Monshi M.R., Modified Scherrer equation to estimate more accurately nano-crystallite size using XRD, World J. Nano Sci. Engineer., 2012, 2(03), 154.
57. Ha H.W., Kim I.Y., Hwang S.J., Ruoff R.S.,One-pot synthesis of platinum nanoparticles embedded on reduced graphene oxide for oxygen reduction in methanol fuel cells,Electrochem. Solid-State Lett. 14(7) (2011) B70-B73.
58. Benedetti J.E., Bernardo D.R., Morais A., Synthesis and characterization of a quaternary nanocomposite based on TiO_2/CdS/rGO/Pt and its application in the photoreduction of CO_2 to methane under visible light, RSC Adv., 2015, 5, 33914-33922.
59. Sharma S., Ganguly A., Papakonstantinou P., Miao X., Li M., Hutchison J.L., Delichatsios M., Ukleja S.,Rapid microwave synthesis of CO tolerant reduced graphene oxide-supported platinum electro catalysts for oxidation of methanol, J. Phys. Chem. C, 2010, 114, 19459-19466.
60. M. Razavian, S. Fatemi, Synthesis and evaluation of seed-directed hierarchical ZSM-5 catalytic supports: inductive influence of various seeds and aluminosilicate gels on the physicochemical properties and catalytic dehydrogenativebehavior, Mater. Chem. Phys. 165 (2015) 55-65.
61. Jamalzadeh Z., Haghighi M., Asgari N., Synthesis, physicochemical characterizations and catalytic performance of Pd/carbon-zeolite and Pd/carbon-CeO_2 nanocatalysts used for total oxidation of xylene at low temperatures, Front. Environ. Sci. Eng., 2013, 7 (3), 365-381.
62. Sun S.H., Yang D.Q., Villers D., Zhang G.X., Sacher E., Dodelet J.P.,Template- and Surfactant-free Room Temperature Synthesis of Self-Assembled 3D Pt Nanoflowers from Single-Crystal Nanowires,Adv. Mater., 2008, 20(3), 571-574.
63. Ye W., Zhang X., Chen Y., Du Y., Zhou F., Wang C., Pulsed Electrodeposition of Reduced Graphene Oxide on Glass Carbon Electrode as an Effective Support of Electrodeposited Pt Microspherical Particles, Int. J. Electrochem. Sci., 2013, 8(2), 2122-2139.
64. Rodriguez J.M.D., Melián J.A.H., Peña J.P., Determination of the real surface area of Pt electrodes by hydrogen adsorption using cyclic voltammetry, J. Chem. Educ., 2000, 9, 1195.
65. Lukaszewski M., Soszko M., Czerwinski A., Electrochemical Methods of Real Surface Area Determination of Noble Metal Electrodes–an Overview, Int. J. Electrochem. Sci., 2016, 11, 4442-4469.
66. Watt-Smith M.J., Friedrich J.M., Rigby S.P., Ralph T.R., Walsh F.C., Nature of the Band Gap of In_2O_3 Revealed by First-Principles Calculations and X-Ray Spectroscopy, J. Phys. D: Appl. Phys., 2008, 100(16), 167402.
67. Singh B., Murad L., Laffir F., Dickinson C., Dempsey E., Pt based nanocomposites (mono/bi/tri-metallic) decorated using different carbon supports for methanol electro-oxidation in acidic and basic media, Nanoscale, 2011, 3(8), 3334-3349.
68. Chung D.Y., Lee K.J., Sung Y.E., Methanol Electro-Oxidation on the Pt Surface Revisiting the Cyclic Voltammetry Interpretation, J. Phys. Chem. C, 2016, 120, 9028-9035.
69. Chatterjee M., Chatterjee A., Ghosh S.,Electro-oxidation of ethanol and ethylene glycol on carbon-supported nano-Pt and -PtRu catalyst in acid solution, Electrochim. Acta, 2009, 54(28), 7299-7304.
70. Wang J., Analytical Electrochemistry, 2nd ed., Wiley, New York, 2000, p. 14.

71. Ehrburger P., Mahajan O.P., Walker Jr. P.L.,Carbon as a support for catalysts: I. Effect of surface heterogeneity of carbon on dispersion of platinum, J. Catal., 1976, 43, 61-67.
72. Flynn P.C., Wanke S.E.,A model of supported metal catalyst sintering: II. Application of model, J. Catal., 1974, 34(3), 400-410.

*****